

IN-SITU MEASURED DYNAMIC RESPONSE OF THE BELL TOWER OF AGIOS GERASIMOS IN LIXOURI-KEFALONIA, GREECE AND ITS UTILIZATION IN THE NUMERICAL PREDICTIONS OF ITS EARTHQUAKE RESPONSE

G.C. Manos¹ and E. Kozikopoulos²

¹ Professor and Director of the Lab. of Strength of Materials and Structures, Aristotle University
e-mail: gcmayos@civil.auth.gr

² Postgraduate student, Lab. of Strength of Materials and Structures, Aristotle University
e-mail: vago_kozi@outlook.com.gr, {dnaxakis@civil.auth.gr}

Keywords: Bell tower, In-situ Dynamic Measurements, Numerical Simulation, Earthquake Response, Soil-structure Interaction.

Abstract. *The dynamic and earthquake response of the bell tower of Agios Gerasimos, located at the city center of Lixouri in the island of Kefalonia, Greece is examined here. This structure was subjected during the winter of 2014 in an intensive earthquake sequence. The dynamic characteristics of this bell tower were measured in-situ through a series of free vibration tests that were performed following the earthquake sequence. Subsequently the dynamic and earthquake response of the bell tower was numerically simulated employing a 3-D elastic numerical simulation shell elements. The foundation was included in the numerical model assumed to be a mass-less concrete block that is formed by mass-less horizontal slabs and vertical slabs. A number of linear horizontal and vertical links are also employed aimed at representing the resistance of the soil surrounding the foundation block in the x-x (N-S), y-y (E-W) and vertical (z-z) directions. The numerical simulation examines the value of the stiffness of these vertical or horizontal links in a parametric way. First, the axial stiffness for all the vertical and horizontal links attains the value of 10000000KN/m that represents a non-deformable soil. Next, the vertical and horizontal links are given a value for their axial stiffness in such a way that the resulting 1st translational E-W (y-y) eigen-frequency is approximately equal to the corresponding value that was measured during the free vibration tests. Then a third case is also examined whereby the stiffness of these links becomes even lower. The obtained numerical results of all these examined cases are presented and discussed. It is demonstrated that the soil – foundation – structure interaction influences the dynamic and earthquake response predictions for this structure quite significantly. It also demonstrates the usefulness of such in-situ testing towards formulating realistic numerical models in order to yield realistic predictions of the dynamic and earthquake response of the examined structures.*

1 INTRODUCTION

The objective of this paper is to study the dynamic and earthquake response of a bell tower. This bell tower belongs to the church of Agios Gerasimos which is located at the city center of Lixouri in the island of Kefalonia, Greece. The whole locality was subjected during the winter of 2014 in an intensive earthquake sequence and this gave the opportunity to focus on the earthquake response of this bell tower which remained unscathed, despite the intensity of the seismic ground motion and the damage to neighboring structures. In figure 1 the location of the Agios Gerasimos bell tower is shown together with the location of the city hall of Lixouri at a distance of 0.35km from the bell tower.



Figure 1. View of the center of Lixouri



Figure 2. The two-story R/C building that housed the City Hall of Lixouri prior to the seismic event of 3rd February 2015. Because of the developed structural damage is not occupied at present.

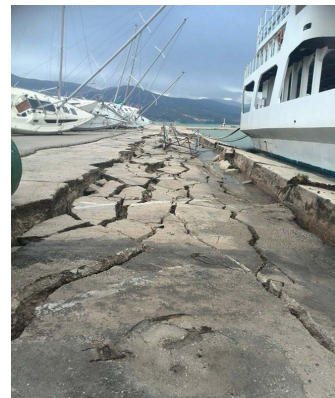


Figure 3. The earth fill embankment at the harbor immediately after the seismic event of 3rd February 2015

The Lixouri City Hall is also shown in figure 2, a two-story reinforced concrete building, developed light structural damage during the 3rd of February 2014 strong seismic ground motion. Similarly, the columns of another two-story reinforced concrete building were also damaged, namely hotel Palatino shown at the left side of figure 1. It is interesting to note that the

intensity of shaking during this damaging 3rd of February 2014 seismic event was recorded by a strong motion accelerograph located at the ground floor of the city hall building [1]. Moreover, spectacular damage was observed at the earth fill embankment [1] that forms the harbor of Lixouri (shown at the bottom of figure 1) as well as the overturning of boats that were free standing at the sea front of this harbor (figure 3).

Bell towers are structures that are of particular interest regarding their dynamic and earthquake response, which has been the subject of research in the past. A large number of bell towers with dimensions much larger than the one examined here are located in numerous cities in Italy and elsewhere. The largest percentage of these bell towers is built by stone or brick masonry. One of the well known cases of a bell tower collapse is that of the St. Marcus bell tower in Venice in July 1902 depicted in figures 4. The Campanile of St. Mark's Church, ninety-eight meters high, collapsed at 10:41 o'clock Monday morning and fell with a great crash into the piazza. The Campanile, which was entirely detached from the cathedral, collapsed where it stood in a heap of ruins (figure 5). This collapse was not due to an earthquake excitation.



Figure 4-5. The Collapse of St. Mark's Bell Tower in Venice in 1902.



Figure 6-7. Torre dei Modenesi, Emilia-Romagna earthquake, May 2012

However, in many other cases earthquake activity constitutes the major cause of serious damage for bell towers that many times leads to partial or total collapse. These structures are characterized with considerable height, relatively to their narrow foundation, and considerable masses along their height; these facts together with the added weight from heavy bells at high elevations lead to large overturning moments and shear forces at their base. There are numer-

ous examples of bell towers that were heavily damaged or collapsed due to earthquake activity. Relatively recently, a 6.0 magnitude earthquake in the region of Emilia-Romagna of Italy caused the collapse of an old tower in the town of Finale Emilia on May 20, 2012. Torre dei Modenesi, a 13th century clock tower was destroyed during this earthquake (figure 6-7). An extensive effort was made by volunteers from all across the country to help salvage, collect and catalogue fragments of the 32-meter high tower in an effort to eventually restore it. On October 16th 2013, a 7.2 magnitude earthquake shook Bohol province in the central Philippines. The Basilica Minore del Santo Niño established in the 1500s and rebuilt in its present form in 1737. The earthquake caused the collapse of its bell tower and portions of its main building, the bell tower of the Church of San Pedro Apostol in Loboc, Bohol that collapsed during the same earthquake.



Figure 8-9 . The Basilica Minore del Santo Niño



Figure 10. The bell tower of the Church of San Pedro Apostol.

Consequently, there is a major international concern for the stability of numerous bell towers. This resulted to significant international research effort that includes in-situ monitoring of the response of bell towers on a temporary basis, like the one attempted here, or more sophisticated and on a permanent basis ([4, 6, 7, 8, 9, 12, 13, 14, 15, 16, 17, 18, 20]). Foundation problems for bell towers are evident in many case the most celebrated being Pisa's grand bell tower in Italy (figure 11) that is quoted as a major medieval engineering error. The two leaning bell towers in Bologna in Italy Another represent another example (figure 12). Therefore, the soil flexibility is also an area of research interest for these structures especially when their dynamic and earthquake response is under investigation [5, 16, 17, 18, 20].



Figure 11. Pisa's grand bell tower



Figure 12. Two leaning bell towers in Bologna



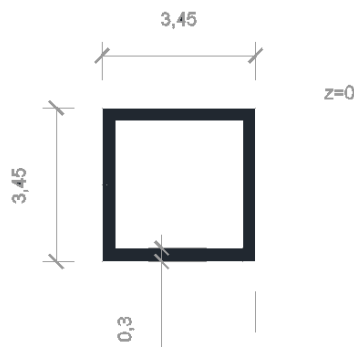
East view of the bell tower



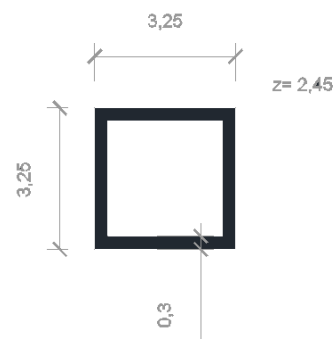
West view of the bell tower

Figure 13-14. Pictorial view of the Agios Gerasimos bell tower (September 2014)

The bell tower that is studied here is depicted in figures 13-14. The height of this bell tower is approximately 20m and it is made of reinforced concrete with a hollow cross-section that has dimensions 3.45m by 3.45m at the ground level and it keeps being reduced along the height, as shown in figures 15-16.



Cross section and dimensions in meters of the bell tower at ground level



Cross section and dimensions in meters of the bell tower at a height of 2.45m from ground level

Figure 15-16. Horizontal cross sections of the bell tower at two different elevations

The walls of the bell tower are made of reinforced concrete with a thickness equal to 300mm. This bell tower was constructed during 1963, almost ten years after the damaging earthquake sequence of 1953 that hit this region [2]. Its foundation consists of a reinforced concrete foundation block that extends at a depth of at least 3.0 meters below ground level. Initially, summary results are presented in section 2 based on measurements of the dynamic response of this bell tower obtained during an in-situ experimental campaign conducted for this purpose on September 2014. Next, the dynamic response of this bell tower is also predicted through a 3-D numerical simulation. From the comparison between the measured and the numerically predicted dynamic response the influence of the soil-foundation interaction is studied and is presented in section 3. Based on the outcome of this comparison the numerical simulation that yield the best predictions is next being utilized to predict the earthquake re-

sponse of this structure during the main event of February 3rd, 2015 [1]. The relevant results are presented in a summary form section 4 together with the final conclusions.

2 IN-SITU MEASUREMENT OF THE DYNAMIC RESPONSE OF THE BELL TOWER

The dynamic characteristics of this bell tower were measured in-situ through a series of free vibration tests that were performed following the damaging earthquake sequence 3rd of February 2014 seismic. A set of two tri-axial accelerometers were utilized together with a digital data acquisition system. These accelerometers were fixed at two locations along the height of the bell tower. The first accelerometer was fixed on a horizontal reinforced concrete (R/C) slabs which was built internally on this bell tower and was connected in a monolithic way with all four peripheral R/C walls. This R/C slab was immediately below the bells and could be reached through a R/C staircase which was also built internally and was also connected in a monolithic way with the peripheral R/C walls. This R/C slab was located at 15.4m from the ground level, which is named here “High Measuring Point (up)” and the accelerometer fixed at this level is depicted in figures 17-18. The second tri-axial accelerometer was also fixed internally on the West R/C wall at a location 11.5m from ground level, which is named here “Low Measuring Point (down)”. This instrumentation arrangement is also shown in figure 19 where it can be seen that both instruments were located at an axis of symmetry of this structure named y-y in figure 19 (East-West).



Figure 17-18. Accelerometer fixed at “High Measuring Point (up)”.

The bell tower was excited by a pull-out free vibration test sequence ([4, 6, 7, 8, 9, 12, 13, 14, 15, 16, 17, 18, 20]) utilizing a sudden rupture of a high strength wire that was previously stretched being attached at on end at the bell tower just above the “High measuring point” level at the other end on a reaction point at the street level that passed near the South side of the bell tower and was accessible for this purpose. This is depicted schematically in figures 20 and 21. As can be seen in figure 21 the excitation axis was at an angle of 14.7 degrees with the East-West axis of symmetry (y-y). As a result, and despite the structural symmetry, it was expected that the dynamic acceleration response of the bell tower for this excitation would be developed both in the y-y as well as in the x-x (North-South) direction.

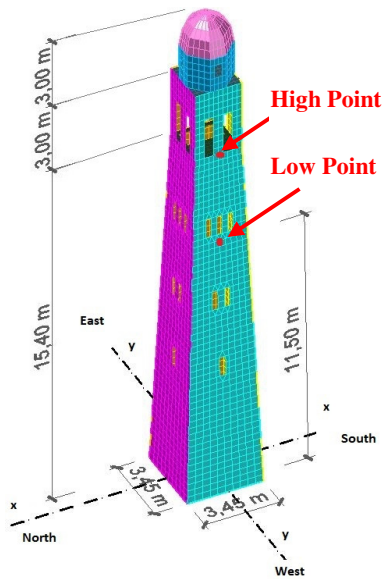


Figure 19. Used instrumentation



Figure 20. Pull-out free vibration test sequence

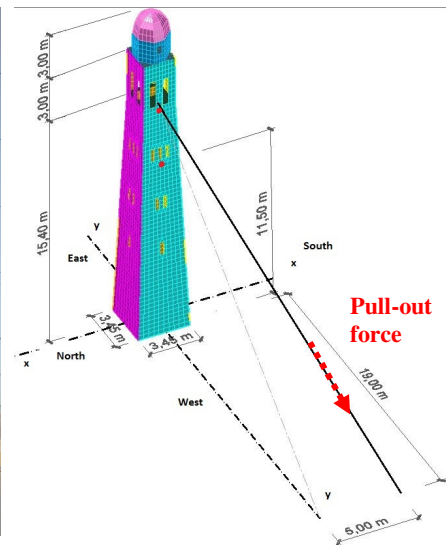


Figure 21. Used pull-out excitation

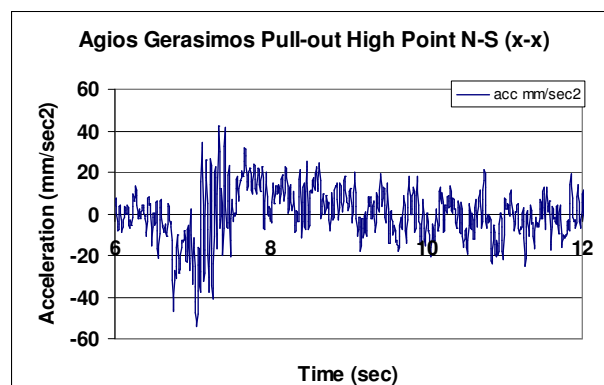
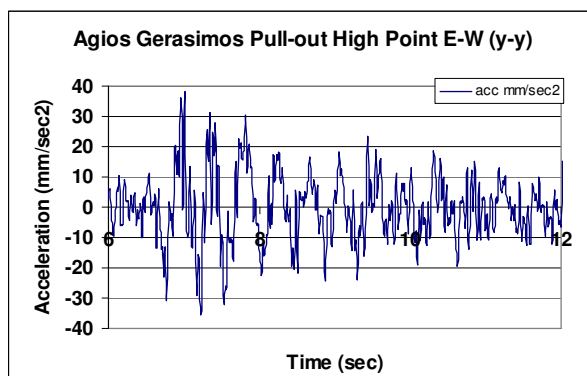


Figure 22-23. Free vibration horizontal acceleration response at the “High measuring point” of the bell tower

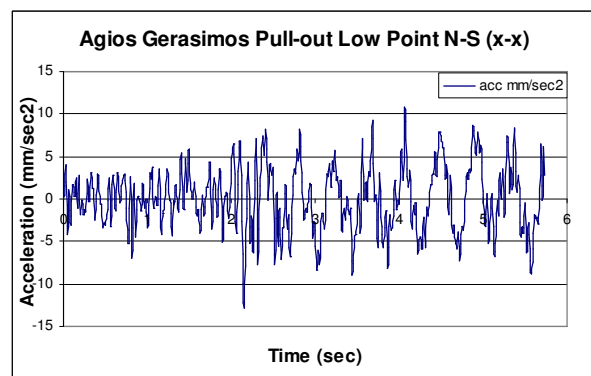
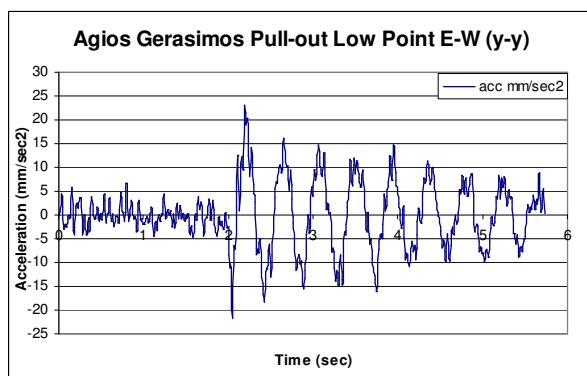


Figure 24-25. Free vibration horizontal acceleration response at the “Low measuring point” of the bell tower

Because the used instruments were tri-axial the response in these two horizontal directions $x-x$ and $y-y$ could be recorded simultaneously and are depicted in figures 22-23 and 24-25 for the “High and Low measuring points”, respectively. As can be seen, the presense of a quite dominant frequency is quite clear in all these free vibration dynamic acceleration responses. This dominant response frequency was extracted from transforming the obtained

measurements in the frequency domain through a fast fourier transform (FFT) algorithm. The following table 1 lists the results of this FFT frequency analysis of the obtained measurements.

Table 1. Peak values from FFT frequency analysis of the East-West (y-y) free vibration acceleration response of the bell tower

	Frequency (Hz)	Period (sec)	FFT amplitude	FFT Phase (rad)	FFT phase adjusted (rad)	Phase Difference Up-down (deg) FFTup/FFTdown
	Agios Gerasimos High measuring point Test 006 (pass filter 0.1Hz-25Hz)					
High Point	2.344	0.427	30.32(up)	-1.411	1.365	0 / 1.789
	Agios Gerasimos Low measuring point (down) Test 006 (pass filter 0.1Hz-25Hz)					
Low point	2.342	0.427	19.627	1.365	1.365	0

The peak FFT values of the East-West free vibration acceleration response of the bell tower are listed in this table together with the measured in this way dominant frequency which is equal to 2.343Hz (0.427 sec. period). Moreover, it can be seen in this table that the peak acceleration response at this dominant vibration frequency is at phase for the two “High and Low measuring points”

3 NUMERICAL SIMULATION OF THE FREE VIBRATION RESPONSE OF THE BELL TOWER

The dynamic response of the bell tower was numerically simulated employing a linear elastic dynamic analysis utilizing shell elements assumed to be of reinforced concrete as an isotropic material with a Young's Modulus equal to $E=10000\text{MPa}$ and typical to reinforced concrete. The bells were assumed to weight 500kg. They were simulated with a steel beam that was placed at the right location and height where the actual steel beam supporting the bells is located. A mass and weight multiplier was used for this beam to account for the extra mass and weight of the bells.

The foundation was assumed to be a mass-less concrete block that was numerically formed by the following parts:

- Two mass-less and stiff horizontal slabs with a thickness 0.15m were located one at the ground level and the other at a depth of 3.0m from the ground level. These slabs represent the upper and lower horizontal planes of the foundation concrete block. In addition, four mass-less and stiff vertical slabs having a thickness 0.789m were also added. Two of these slabs were placed at the x-z plane and the other two at the y-z plane of the numerical model. These vertical slabs represent the peripheral vertical planes of the foundation block facing the East-West (x-z plane) and the North-South (y-z plane) directions. In this way the foundation block was formed (figure 26). All the stiffness properties of the finite elements representing these slabs were numerically increased by a multiplier equal to 1000.

- Next, four mass-less and weightless stiff vertical slabs were also formed parallel to the previously described vertical slabs. These later vertical slabs were placed in a way surrounding externally the foundation block. They were located at a distance of 50mm externally surrounding the vertical slabs representing the foundation block. An additional mass-less and

weightless stiff horizontal slab was also added placed 50mm below the horizontal slab that represents the bottom of the foundation block (-3.0m from the ground level). All these slabs, both vertical and horizontal are presumed to represent the non-deformable support medium for the foundation block of the bell tower, and for this purpose they were considered to be practically non-deformable as well as they were constrained at all their nodes in the x-y-z direction.

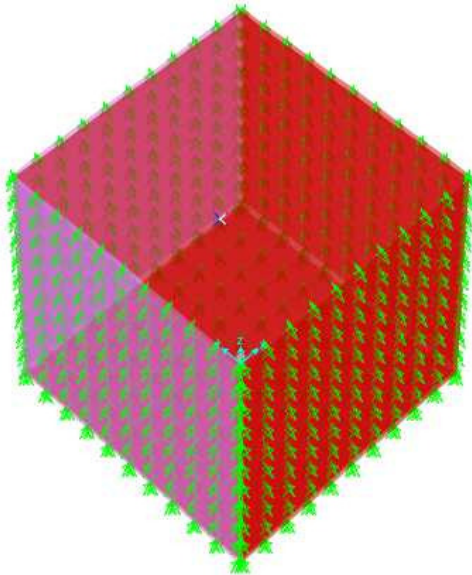


Figure 26. Numerical simulation of the foundation block

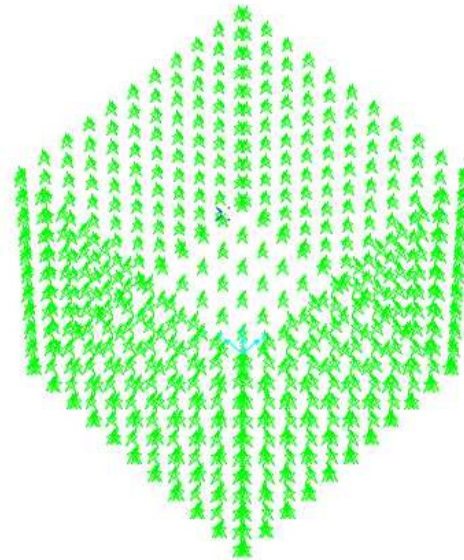
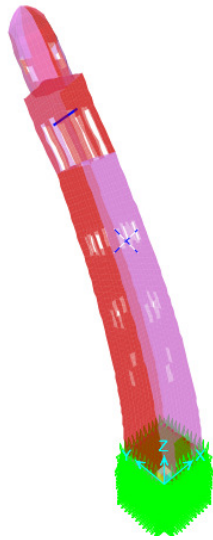


Figure 27. Numerical simulation of the soil-foundation interaction with links

- In order to account for the soil deformability the rigid slabs representing the non-deformable supports of the foundation block were connected to the corresponding vertical and horizontal slabs representing all the sides of the foundation block in contact with the surrounding soil with two-node links (figure 27). These two-node links were placed within the space that was left in the numerical model between the non-deformable support slabs and the non-deformable foundation slabs. In this way, all the foundation soil interaction that could arise from the soil deformability was concentrated locally on these two-node links at the 50mm space left for this purpose surrounding the numerical model of the foundation block from all its sides.

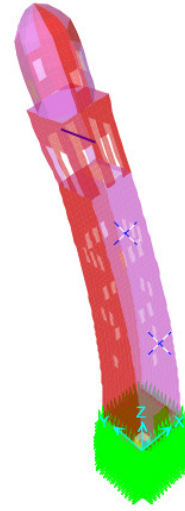
- Three cases were considered regarding the value of the stiffness of these vertical or horizontal links. In the first case the axial stiffness for all the vertical and horizontal links attains the value of 100000000KN/m. That represents a non-deformable soil. In the second case all the vertical and horizontal links are given a value for their axial stiffness in such a way that the resulting 1st translational E-W (y-y) eigen-frequency of the bell tower is approximately equal to the corresponding value that was measured during the free vibration tests. The axial stiffness value for all the links in this case was found to be equal to 21000KN/m. This was assumed to represent medium stiffness conditions for the soil.

Deformed Shape (MODAL) - Mode 1; T = 0.23483; f = 4.25847



Translational mode E-W (y-y)
T=0.235 sec., f=4.258Hz (rigid soil)

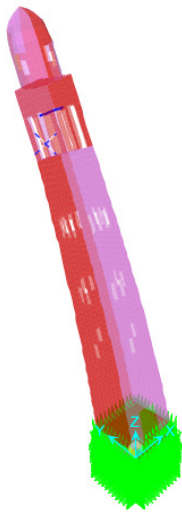
Deformed Shape (MODAL) - Mode 2; T = 0.22916; f = 4.36376



Translational mode N-S (x-x)
T=0.229, f=4.364Hz (rigid soil)

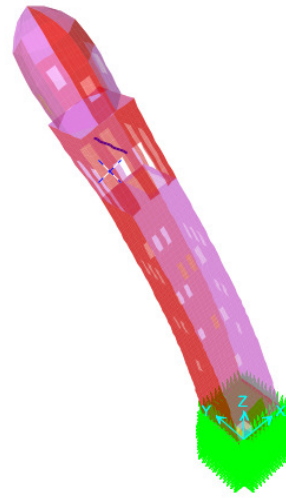
Figure 28-29. Predicted translational mode for the first examined soil condition (rigid soil)
Axial link stiffness 10000000KN/m

Deformed Shape (MODAL) - Mode 1; T = 0.42672; f = 2.34345



Translational mode E-W (y-y)
T=0.4267sec., f=2.343Hz, (medium soil)

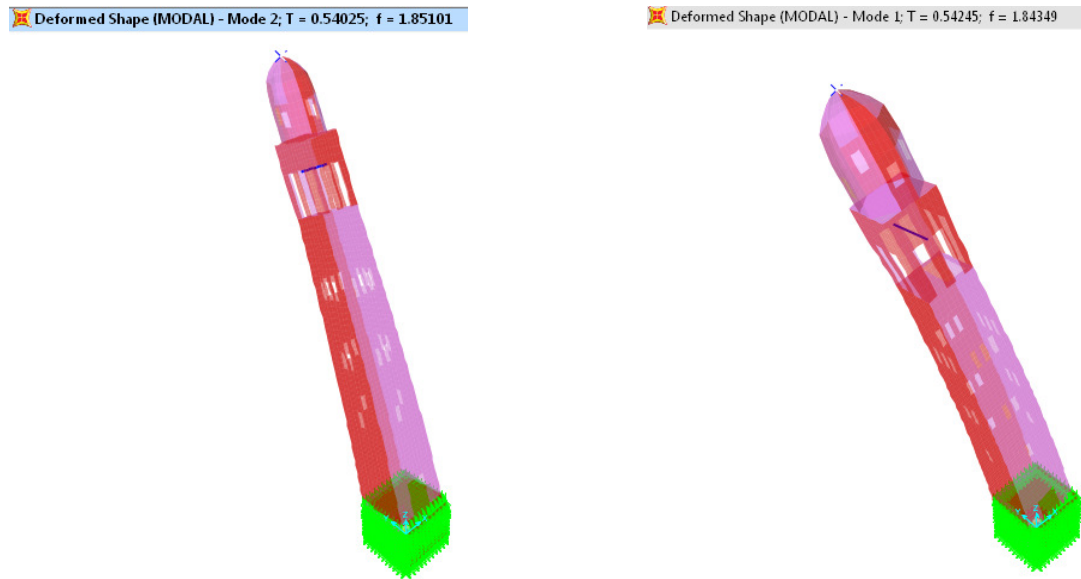
Deformed Shape (MODAL) - Mode 2; T = 0.42543; f = 2.35059



Translational mode N-S (x-x)
T=0.4254, f=2.351Hz, (medium soil)

Figure 30-31. Predicted translational mode for the first examined soil condition (medium soil). Axial link stiffness 21000KN/m

The excitation introduced by the free vibration tests that were performed in-situ should be considered as a rather low intensity excitation. Therefore, the soil surrounding the foundation is presumed to have stiffness properties that may be reduced when subjected to an intense excitation during a prototype earthquake ground motion like the one experienced during the damaging 3rd of February 2014 seismic event at Lixouri. For this purpose, a third case of axial link stiffness was also considered. In this third case the axial stiffness value for all the links was set equal to 10000KN/m. The values of the predicted eigen-frequencies / eigen-periods for the dominant translational modes for the examined three soil conditions of the Agios Gerasimos bell tower are shown in figures 32 to 33 and listed in table 2.



Translational mode E-W (y-y)
T=0.540sec., f=1.851Hz, (flexible soil).

Translational mode N-S (x-x)
T=0.542, f=1.843Hz, (flexible soil).

Figure 32-33. Predicted translational mode for the first examined soil condition (flexible soil). Axial link stiffness 10000KN/m

Table 2. predicted eigen-frequencies / eigen-periods for the dominant translational modes for the examined three soil conditions of the Agios Gerasimos bell tower

Soil Foundation deformability	Predicted East-West translational mode eigen-frequency (Hz) / eigen-period (sec)	Predicted North-South translational mode eigen-frequency (Hz) / eigen-period (sec)
1 st case Rigid Soil Axial stiffness for links 10000000KN/m	4.258Hz / 0.235sec.	4.364Hz / 0.229sec.
2 nd case Medium Soil Axial stiffness for links 21000KN/m	2.343Hz / 0.4267sec.	2.351Hz / 0.4254sec.
3 rd case Flexible Soil Axial stiffness for links 10000KN/m	1.851Hz / 0.540sec.	1.843Hz / 0.542sec.

As already mentioned, the objective of this parametric study of soil-deformability was to be able to investigate the sensitivity of the fundamental dynamic properties of this bell-tower that arises from the deformability of the soil-foundation [5, 10, 16, 17, 18, 20]. In the table that follows the values of the measured eigen-frequencies / eigen-period that were obtained from the in-situ free vibration dynamic measurements are compared with the corresponding predicted values for the three soil-foundation conditions.

As can be seen from the eigen-frequency / eigen-period values listed in table 3, the predictions obtained through the bell tower numerical simulation employing deformable linear links at the interface between the foundation and the soil, as was described in this section, demonstrate very good agreement with the measured values for the 2nd case representing a medium flexibility soil which is approximated in the numerical simulation through an axial stiffness value for the links equal to 21000KN/m.

Table 3. predicted eigen-frequencies / eigen-periods for the dominant translational modes for the examined three soil conditions of the Agios Gerasimos bell tower

Soil Foundation deformability	Predicted 1 st case Rigid Soil	Predicted 2 nd case Medium Soil	Predicted 3 rd case Flexible Soil	Measured values
Axial stiffness for links	10000000KN/m	21000KN/m	10000KN/m	--
East-West translational mode eigen-frequency (Hz)/ eigen-period (sec)	4.258Hz / 0.235sec.	2.343Hz / 0.4267sec.	1.851Hz / 0.540sec.	2.343Hz / 0.4268sec.
North-South translational mode eigen-frequency (Hz) / eigen-period (sec)	4.364Hz / 0.229sec.	2.351Hz / 0.4254sec.	1.843Hz / 0.542sec.	2.344Hz / 0.4266sec.

4 EARTHQUAKE RESPONSE OF THE AGIOS GERASIMOS BELL TOWER

Next, the numerical simulation of the earthquake response of the Agios Gerasimos bell tower for the previously presented three cases of soil-foundation deformability was examined. In this investigation the following load case combinations were considered in an effort to approximate the seismic forces that this structure was subjected to during the 3rd of February 2015 actual earthquake excitation.

1. The gravity loads is signified as DEAD. It represents all the vertical gravity forces that are generated from the weights of all the structural and the non-structural components of the bell tower including the bells themselves. All the inclined R/C walls of the tower were considered to have a thickness of 0.3m. The 3-D shell F.E. representation follows the middle plane of these walls. From the level upwards from the upper slab (below the bells) the wall are vertical till the level of the upper dome. The top of the dome rises 21.4m from the ground level. All the window and door openings are replicated in the F.E. model.

2. The horizontal seismic loads in the y-y (E-W) direction are applied in a static way. They are approximated as being 50% of the vertical gravity forces acting horizontally in the x-x direction. These loads are denoted as 0.5 E_y (E-W) static and together with the vertical gravity forces (DEAD) represent combination 1. Thus COMBI-1 = DEAD + 0.5 E_y (E-W). In a similar way, the horizontal seismic loads in the x-x (N-S) direction are also applied in a static way. They are approximated as being 50% of the vertical gravity forces acting horizontally in the x-x direction. These loads are denoted as 0.5 E_x (N-S) static and together with the vertical gravity forces (DEAD) represent load-combination 2. Thus COMBI-2 = DEAD + 0.5 E_x (N-S)

3. Alternatively, The horizontal seismic loads in the y-y (E-W) direction are applied through the Lixouri E-W elastic acceleration response spectral curve for 5% damping ratio as it was derived from the E-W component of the acceleration record that was recorded during the strong aftershock of 3-2-2014 ([1]). This was recorded by an instrument located at the ground floor slab of a R/C two-story building (Dimarchion) located at a distance of 350m from the bell tower, as indicated in figure 1. This response spectrum values are scaled to ac-

count for a response modification factor with a value equal to 2.5. This value must be considered as rather high value based on the fact that the bell tower is a cantilever and there were no visible signs that the reinforced concrete sections with their reinforcing bars were stressed to post-yield levels. Due to these reasons it is expected that the response of the bell tower predicted by dividing the response spectra curve by $\mu=2.5$ will be rather low than what this bell tower could possibly have experienced during the actual seismic event according to the recorded ground acceleration. These seismic loads are denoted as E-W response spectrum and together with the vertical gravity forces (DEAD) represent load-combination 3. Thus COMBI-3 = DEAD + E-W Response spectrum.

As already mentioned, figure 34 depicts the East-West constant ductility acceleration response spectral curve, for damping ratio equal to 5% of critical and for ductility factor $\mu=2.5$, together with the Euro-code 8 design spectral curves (Type 1 and Type 2) for soil category D (flexible soil) for design ground acceleration equal to 0.36g (g the acceleration of gravity), for importance factor $\gamma=1$, and for response modification factor $q=3$ [21]. In the same figure the acceleration spectral values corresponding to the measured and predicted eigen-periods values listed in table 3 for the three examined soil conditions are also indicated. The acceleration spectral value indicated in this figure as L.P.T. corresponds to the lowest eigen-period value of the bell tower for the 1st case of rigid soil conditions. The acceleration spectral value indicated in this figure as “measured” corresponds to eigen-period value of the bell tower for the 2nd case of medium soil conditions that also coincides with the measured value during the in-situ tests described before. Finally, the acceleration spectral value indicated in this figure as H.P.T. corresponds to the highest eigen-period value of the bell tower for the 3rd case of flexible soil conditions.

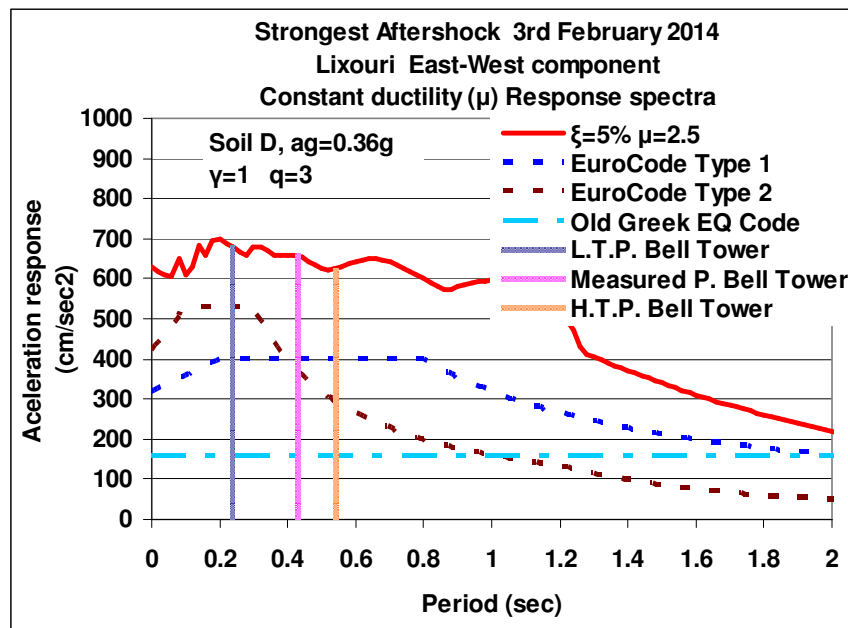


Figure 34. East-West acceleration spectral values for the examined cases of soil conditions for the bell tower

4. The horizontal seismic loads in the x-x (N-S) direction are approximated in a similar way as the one described below utilizing the Lixouri N-S elastic acceleration response spectral curve for 5% damping ratio as it was derived from the N-S component of the acceleration record that was recorded during the strong aftershock of 3-2-2014 [1]. These loads are denoted as N-S response spectrum and together with the vertical gravity forces (DEAD) represent loadcombination 4. Thus COMBI-4 = DEAD + N-S Response spectrum.

Figure 35 depicts the North-South constant ductility acceleration response spectral curve, for damping ratio equal to 5% of critical and for ductility factor $\mu=2.5$, together with the Euro-code 8 design spectral curves (Type 1 and Type 2) for soil category D (flexible soil) for design ground acceleration equal to 0.36g (g the acceleration of gravity), for importance factor $\gamma=1$, and for response modification factor $q=3$ [21]. In the same figure the acceleration spectral values corresponding to the eigen-period values of table 3 are plotted again here with the same symbols.

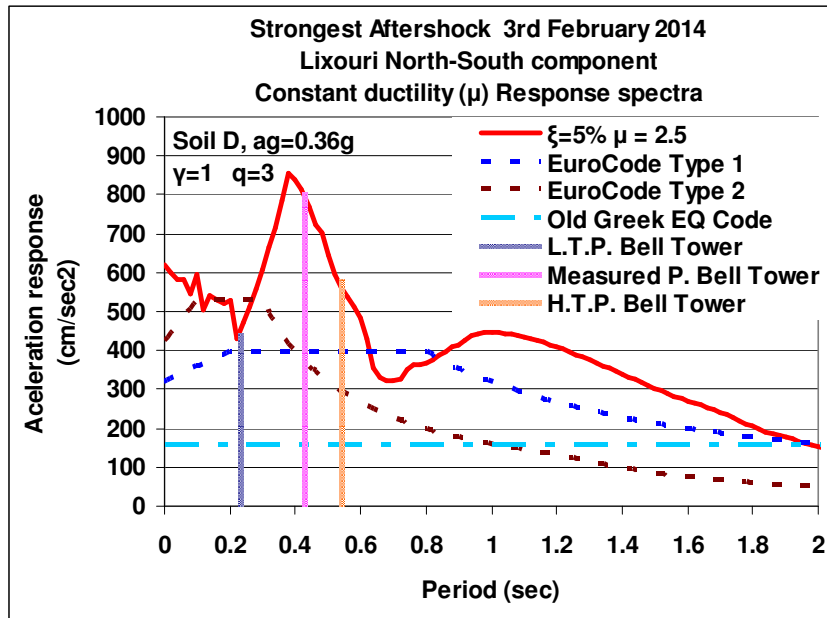


Figure 35. North-South Acceleration spectral values for the examined cases of soil conditions for the bell tower

5. Finally, the horizontal seismic loads in the y-y (E-W) direction are applied through the the E-W component of the acceleration record that was recorded during the strong aftershock of 3-2-2014. This is denoted as E-W time history. Similarly, the horizontal seismic loads in the x-x (N-S) direction are applied through the N-S component of the acceleration record that was recorded during the strong aftershock of 3-2-2014. This is denoted as N-S time history. Both these forcing actions together with the vertical gravity forces (DEAD) represent combination 5. Thus COMBI-5 = DEAD + E-W time history + N-S time history. For all these acceleration forcing actions no scaling was introduced as was done for the horizontal forces based on the response spectral curves that were applied in the way explained before. The step-by-step direct integration method was used for these time history dynamic analyses. For the case of flexible soil damping was introduced at all the vertical and horizontal links with the value of 10% of critical. This increase in the damping ratio value was introduced in order to mitigate the resulting earthquake response for this loading case and to account up to a point the radiation damping that would be introduced in this case from the soil-foundation interaction.

The following observations can be deduced from figures 34 and 35.

- a) For almost all the examined soil conditions the acceleration spectral values of the bell tower are considerably higher than the corresponding values of the Euro-code [21] (either type 1 or 2). The only exception is the spectral acceleration value for the rigid soil condition and for the type 2 Euro-code design spectral curve. This means that in

almost all cases the actual seismic loads that this structure experienced during this particular earthquake are larger than the design seismic loads even if this bell tower was designed with the current earthquake loads, as these are specified by Euro-code 8.

- b) The previous remark becomes even more outstanding if one uses for comparison the level of design seismic loads that was specified by the old Greek seismic code design acceleration levels which are also indicated in figures 34 and 35 [11]. It must be pointed out here that during the period that this structure was designed and constructed the seismic loads generally considered were those indicated in figures 34 and 35 as “Old Greek EQ Code” [11].

Table 4. Maximum base shear and horizontal displacement at the top of the bell tower

Load Combination	1 st case Rigid soil		2 nd case Medium soil		3 rd case Flexible soil	
	Base Shear (KN)	Top Displ. (mm)	Base Shear (KN)	Top Displ. (mm)	Base Shear (KN)	Top Displ. (mm)
Combination 1 D + static (E-W)	Qy=633	Uy=11.7	Qy=633	Uy=38.8	Qy=633	Uy=61.2
Combination 2 D + static (N-S)	Qx=633	Ux=12.4	Qx=633	Ux=38.7	Qx=633	Ux=62.2
Combination 3 D + R. Spectrum (E-W)	Qy=344	Uy=12.4	Qy=511	Uy=36.6	Qy=380	Uy=52.8
Combination 4 D + R. Spectrum (N-S)	Qx=278	Ux=9.1	Qx=438	Ux=37.6	Qx=324	Ux=44.7
Combination 5 D + Time history (N-S) +Time history (E-W)	Qx=754 Qy=1096	Ux=18.8 Uy=25.2	Qx=1246 Qy=1249	Ux=102.5 Uy=88.3	Qx=839 Qy=1218	Ux=107.8 Uy=139.2

Table 4 lists the maximum (minimum) values of the earthquake response of the bell tower for all five examined load combinations as they were previously described. The listed values correspond to the base shear and to the horizontal displacements (U_x / U_y) at the top of the bell tower at a height equal to 21.4m from ground level. From the values listed in this table the following remarks can be made:

a1) As can be seen from the values listed in table 4 the most demanding load combination for all three cases of soil flexibility is load combination 5 where the dead load is combined with the two horizontal acceleration time histories of the ground motion in the East-West and North-South direction recorded at the top surface of the foundation slab of the 2-story City Hall R/C building located 350m away from the bell tower. This increase in the earthquake response of the bell tower when load combination 5 is employed becomes significantly enlarged for medium and flexible soil conditions.

b1) For load combinations 3, 4 and 5 that take into account the dynamics of the studied structure the flexibility of the soil resulted in larger response in terms of base shear. This increase in the value of the base shear must be attributed to the variation of the fundamental period of the structure with the soil flexibility combined with the characteristics of this earthquake ground motion, which can also be seen in the shape of the spectral curves depicted in figure 34 and 35.

c1) The very noticeable increase in the amplitude of the horizontal displacement at the top of the bell tower when the soil conditions become relatively flexible is partly due to the corresponding increase of the horizontal seismic forces resulting from the variation of the soil deformability, as discussed in b1 before, as well as to a component of the horizontal

displacement at the top of the bell tower resulting from the rocking of the foundation block. Obviously, this rocking tends to increase when the flexibility of the foundation becomes larger [20].

d1) This investigation is under process in order to examine further the implications of the structure-foundation-soil interaction as well as the structural performance of the bell tower. For the later task a more detailed investigation is needed in order to ascertain important structural details of this bell tower.

5 CONCLUSIONS

- It was demonstrated by the in-situ measurements of the dynamic response of the Agios Gerasimos bell tower that the foundation deformability is a significant parameter that must be taken into account in order for the numerical response predictions to have any realism.
- It was also demonstrated that for these measured fundamental eigen-period values the bell tower has been subjected to seismic loads higher than the ones specified by the current Euro-code 8 provisions.
- Furthermore, it was shown that for these measured fundamental eigen-period values the bell tower has been subjected to seismic loads considerably higher than the ones specified by the “Old Greek Seismic Code” provisions that were valid at the time of its design and construction.
- From the numerical prediction of the earthquake response of this bell tower based on the actual the earthquake ground motion recorded at a very close distance it was shown that the soil flexibility results in both an increase of the seismic loads as well as in a considerable increase of the resulting horizontal displacements that apart from the increase in the seismic loads bear also the outcome of the rocking response of the foundation block.
- In situ measurements like the ones presented here are very important to be able to identify sources that may significantly influence the dynamic and earthquake response of civil engineering structures. They may also serve the purpose to help formulate a realistic numerical model by properly incorporating such influences in order to yield realistic predictions of the dynamic and earthquake response of the examined structure.

ACKNOWLEDGEMENTS

The authors would like to thank Civil Engineer D. Naxakis for his assistance during the in-situ measurements. Moreover, we would like to thank the priest of the church of Agios Gerasimos at Lixouri, Kefalonia-Greece, father Athanasios Likoudis, for all the information he has provided.

REFERENCES

- [1] GEER - EERI - ATC - Cephalonia GREECE *Earthquake Reconnaissance January 26th/ February 2nd 2014 Version 1: June 6 2014*
- [2] Papazachos, B. and Papazachou, K., 1989, 1997, 2003. The earthquakes of Greece, *Zitis Publ.,Thessaloniki*, 356 pp., 304 pp., 286 pp. (in Greek).
- [3] L. de Stefani, R. Scotta, M. Lazzari, A. Saetta. Seismic improvement of Slender Bell Tower and Minarets. – *PROHITECH, Antalya, Turkey, 2014*
- [4] R. M. Azzara, L. Zaccarelli, A. Morelli, T. Trombetti. Seismic Monitoring of the Asinelli and Garisenda Medieval Towers in Bologna (Italy), an Instrumental Contribution to the Engineering Modeling Directed to their Protection. - *PROHITECH, Antalya, Turkey, 2014*
- [5] Casolo Siro, Uva Giuseppina. Non-Linear dynamic analysis of masonry towers under natural accelerograms accounting for soil-structure interaction. – *COMPDYN 2013 - Kos Island, Greece, June 12-14, 2013*
- [6] A. Saisi, C. Gentile, L. Cantini. Post – Earthquake assessment of a masonry tower by on – site inspection and operational modal testing. – *COMPDYN 2013 - Kos Island, Greece, June 12-14, 2013*
- [7] D. Colapieto, A.Fiore, A. Netti, F. Fatiguso, G Marano, M. de Fino D. Cascella, A. Antona. Dynamic identification and evaluation of the seismic safety of a masonry bell tower in the south Italy. – *COMPDYN 2013 - Kos Island, Greece, June 12-14, 2013*
- [8] R. Guidorzi, R. Diversi, L.Vincenzi, C. Mazzotti, V. Simioli. Structural monitoring of the Tower of the Faculty of Engineering in Bologna using MEMS –based sensing. – *EURODYN 2011 – Leuven, Belgium, 4-6 July 2011*
- [9] C. Blasi M. Carfagni, S. Carfagni. The use of impulsive actions for the structural identification of Slender monumental buildings- *STREMAH-1991 - Seville, Spain, 14-16 May 1991*
- [10] S. Dumorier, W.P. De Wilde. Finite element study of the Tower of Brussels City Hall – *STREMAH 1995 – Chania, Crete, Greece, 1995.*
- [11] G.C. Manos, Seismic Code of Greece, Chapter 17, International Handbook of Earthquake Engineering: "Codes, Programs and Examples", *edited by Mario Paz, by Chapman and Hall*, ISBN 0-412-98211-0, 1994.
- [12] G.C. Manos, et al. (1996) "Predictions of the dynamic characteristics of a 5-story R.C. building at the Volvi Euro-SeisTest Site, utilizing low-intensity vibrations", *3rd European Conference on Structural Dynamics, Eurodyn 1996, Florence, II*, 877–884.
- [13] G. C. Manos, (1998). "The Dynamic Response of a 5-story Structure at the European Test site at Volvi-Greece." *6th U.S. National Earthquake Engineering Conference, May 31 - June 4, Seattle, Washington, U.S.*
- [14] G. C., Manos, et al.. (2004). "Dynamic and Earthquake Response of Model Structures at the Volvi – Greece European Test Site." *13th World Conference on Earthquake Engineering, Vancouver, Canada.*
- [15] G. C., Manos, V. Kourtides, V.J. Soulis, A.G. Sextos, A. G., and P. Renault, (2006). "Study of the dynamic response of a bridge pier model structure at the Volvi - Greece European

Test Site.” *8th National Conference on Earthquake Engineering, April 18-22, San Francisco, U.S.A.*

- [16] G.C. Manos, V. Kourtides, A. Sextos, P. Renault, S. Chiras “Study of the dynamic soil-structure interaction of a bridge pier model based on structure and soil measurements” *9th Canadian Conf. on Earthquake Engineering, Ottawa, Ontario, Canada, 26-29 June 2007.*
- [17] G.C. Manos, V. Kourtides, A. Sextos, S. Chiras “Soil-Foundation-Bridge Pier Interaction at the Euro-Seis Test Site”, *4th Int. Conference on Geotechnical Engineering, Thessaloniki, 24-28 June, 2007.*
- [18] G.C. Manos, V. Kourtides, A. Sextos, “Model Bridge Pier Foundation- Soil Interaction implementing, in-situ / shear stack testing and numerical simulation”, *14WCEE, Beijing, CHINA, 2008.*
- [19] Manos George, “Consequences on the urban environment in Greece related to the recent intense earthquake activity”, *Int. Journal of Civil Engineering and Architecture, Dec. 2011, Volume 5, No. 12 (Serial No. 49), pp. 1065–1090.*
- [20] G. C. Manos , K.D. Pitilakis, A.G. Sextos, V. Kourtides, V. Soulis, J. Thauampth, “Field experiments for monitoring the dynamic soil-structure-foundation response of model structures at a Test Site” *Journal of Structural Engineering, American Society of Civil Engineers, Special Issue “Field Testing of Bridges and Buildings, D4014012, Vol. 141, Issue 1, January 2015.*
- [21] Eurocode 8: Design of structures for earthquake resistance - Part 1: General rules, seismic actions and rules for buildings, *FINAL DRAFT prEN 1998-1, December 2003.*